Origin of high kurtosis levels in the viscous sublayer. Direct numerical simulation and experiment

C. Xu and Z. Zhang
Department of Engineering Mechanics, Tsinghua University, Beijing, People's Republic of China

J. M. J. den Toonder and F. T. M. Nieuwstadt
Laboratory for Aero and Hydrodynamics, Delft University of Technology, 2628 AL Delft, The Netherlands

(Received 6 July 1995; accepted 11 March 1996)

In the literature, a major discrepancy is reported between the value of the kurtosis for the normal velocity fluctuations close to the wall as found from direct numerical simulations and obtained from experiments. The origin of these high kurtosis levels is analyzed with help of a direct numerical simulation of a turbulent channel flow. In addition, a detailed analysis of LDV measurements in the near-wall region of a turbulent pipe flow is made with the results of the DNS as a starting point. In both data sets, i.e. DNS and experiments, similar velocity events were found that contribute to the high kurtosis level. The dynamics of these events can be associated with the regeneration process of streamwise vortices as described by Brooke and Hanratty [Phys. Fluids A **5**, 1011 (1993)]. Based on this evidence, we conclude that the high kurtosis is of a truly physical nature. It is caused by very strong events that appear only in the near-wall region and that are rare in time as well as in space. The very rare appearance of these events explains why they are usually missed in experimental data which are mostly obtained from averages over a limited time series. In this respect the DNS results may be considered as more accurate because they are based on surface averages. © *1996 American Institute of Physics.* [S1070-6631(96)00707-6]

I. INTRODUCTION

Direct numerical simulation (DNS) is a fully resolved numerical solution of the Navier-Stokes equations that is able to describe the spatial and temporal evolution of turbulent flow in all its details. It provides three-dimensional time-dependent velocity and pressure fields, which allow not only a study of statistical properties of the flow, but it also allows investigation of flow structures in turbulence. During the past decade, DNS has developed into a well-established method to explore turbulence. Notable examples of DNS are the studies by Kim *et al.*[1] (channel flow), Spalart[2] (developing turbulent boundary layer along a flat plate), Lyons *et al.*[3] (channel flow with heat transfer), Kristoffersen and Andersson[4] (rotating channel), Gavrilakis[5] (square duct), and Eggels *et al.*[6] (pipe flow). All these simulations have provided data bases that enable detailed studies and they have contributed much to our present knowledge of turbulence.

A major advantage of DNS over laboratory experiments is, that it leads to information that is very difficult to obtain experimentally. Examples are the statistics of pressure fluctuations, higher-order velocity statistics, and the evolution of vorticity structures. Still, one cannot do without laboratory experiments. They are for instance needed to validate DNS and also to verify the results of subsequent studies carried out with the DNS data. Refinement of existing measurement techniques, e.g. laser doppler velocimetry (LDV), and the development of new techniques such as Particle Image Velocimetry (PIV), have opened up in the past decade possibilities to perform detailed measurements. The investigations of Karlsson and Johansson[7] (boundary layer, LDV), Niederschulte *et al.*[8] (channel flow, LDV), and Durst *et al.*[9] (pipe flow, LDV), have complemented and extended previous experiments such as those of Kreplin and Eckelmann[10] (channel flow, hot film).

In a comparison between the DNS results and experimental data, for the flows listed above, in general good agreement is found for quantities, such as the mean velocity profiles and the turbulence intensities. (Detailed comparisons can be found in Niederschulte *et al.*,[8] Eggels *et al.*,[6] and Durst *et al.*[9]). Also for the higher-order statistical moments of the velocity fluctuations the agreement is generally found to be acceptable. However, there is one major discrepancy. In all numerical simulations, the kurtosis of the normal velocity component F_v shows a steep rise near the wall and reaches very high values in the viscous sublayer, i.e. $y^+ < 5$. Kim *et al.*[1] report a value of $F_v = 22$ at the wall, and Eggels *et al.*[6] find $F_v = 19$. In contrast, all experiments up to date seem to indicate that when the wall is approached, the kurtosis reaches a maximum and thereafter decreases, approaching in the viscous sublayer a value which is close to Gaussian value, i.e. $F_v \approx 3$.

This discrepancy has given rise to various speculations about its background. Possible explanations have been given by Lyons and Hanratty.[3] They argue that the difference of their simulation results with the experimental data of Niederschulte *et al.*[8] might be due to smoothing operations used in analyzing the LDV data. As another possible explanation they suggest that the numerical grid resolution may influence statistics, especially the kurtosis of the normal velocity. They find it also conceivable that the periodic boundary conditions used in the simulations may play some role. Also Durst *et al.*[9] suggest numerical resolution as an explanation for the difference between their measurements of F_v near a pipe wall and DNS results. Nevertheless, all authors

 1070-6631/96/8(7)/1938/7/$10.00

agree that a fully satisfactory explanation still missing, so the issue remains unresolved.

The purpose of this paper is to establish whether the high kurtosis values found in DNS data are numerical artifacts of the computations, or are in fact of a truly physical nature. Our strategy is to study first the origin of the high kurtosis levels in the computations. For this we examine a DNS data base for a turbulent channel flow. With the DNS results as a point of departure, we then analyze data obtained from LDV measurements in the near wall region of a turbulent pipe flow and look for events that according to the DNS results contribute to the high kurtosis values.

The outline of this paper is as follows. In Section II we will briefly describe our DNS code, examine the general properties of the events with high kurtosis levels, and analyze the relation between these events and streamwise vortices. Section III contains a description of our experiments and the results of the LDV measurements. Finally, the conclusions are stated in Section IV.

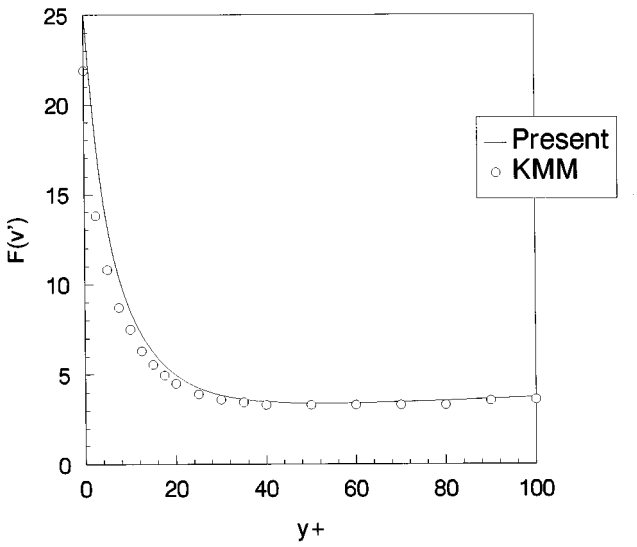

FIG. 1. Kurtosis of the normal velocity fluctuations in a simulated channel flow; comparison of our DNS results (solid line) and those of Kim *et al.* (circles).

II. DIRECT NUMERICAL SIMULATION

A. Description

The high kurtosis events are studied with the help of a DNS data base for the case of a fully developed turbulent channel flow. We have followed largely the methods proposed by Kim *et al.*,[1] so that a short summary of our model will suffice here.

The equations that we solve numerically are

$$\frac{\partial \mathbf{v}}{\partial t} = \mathbf{v} \times \boldsymbol{\omega} - \nabla \Pi + \nu \nabla^2 \mathbf{v}, \tag{1}$$

in combination with the incompressibility constraint

$$\nabla \cdot \mathbf{v} = 0. \tag{2}$$

Here, $\mathbf{v}$ is the velocity vector, $\Pi = \mathbf{v}^2/2 + p/\rho$ the total pressure, ν the kinematic viscosity, ρ the fluid density, and $\boldsymbol{\omega} = \nabla \times \mathbf{v}$ the vorticity.

Equations (1) and (2) are solved numerically by means of a spectral method which employs Fourier functions in the homogeneous direction parallel to the channel walls and Chebyshev polynomials for the non-homogeneous direction between the walls. A time-splitting method with third-order accuracy is used for time advancement. Aliasing errors in the streamwise and spanwise directions are removed by a spectral truncation method (also referred to as the 3/2-rule). For further information, such as regarding boundary and initial conditions, we refer to Kim *et al.*[1]

The resolution of our computation is $128 \times 129 \times 128$ in the streamwise, normal and spanwise directions, respectively. The Reynolds number is $\mathrm{Re}_m = 2666$ (based on the channel half width H and the bulk mean velocity U_m), which corresponds to $\mathrm{Re}_\tau = 172$ (based on H and the friction velocity u_τ). The size of the computational domain in the streamwise and spanwise direction was chosen to be $4\pi H$ and $2\pi H$, respectively (i.e. 2150 and 1070 in wall units). The corresponding gridsize in the streamwise direction is $\Delta x^+ \approx 17$ and in the spanwise direction $\Delta z^+ \approx 8$. The maximum spacing in the normal direction is found at the channel centerline and measures about 4.3 wall units. The minimum normal grid space is near the wall with the first gridpoint from the wall at $y^+ \approx 0.05$. There are 15 gridpoints in the normal direction within the first 10 wall units from the wall so that the viscous sublayer is well resolved. The time step used is $\Delta t = 0.01 H/U_m$.

The computation has been carried out on the Cray-YMP4/464 computer of the Academic Computing Services Center (SARA) at Amsterdam. The memory required was about 58 Mwords (= 464 Mbytes). Each complete time step took about 10 CPU-seconds. The total CPU-time was about 100 hours.

The turbulence statistics that we have computed from our simulation data, are found to be in good agreement with the results of Kim *et al.*[1] As an example we give in Fig. 1 our results for the kurtosis of the normal velocity fluctuations together with the data of Kim *et al.*[1] The difference between the two results can be considered as small if we take into account the following facts. First, the statistical accuracy decreases for higher-order moments such as the kurtosis. Second, as we will see in the following section, the high kurtosis levels are determined by small spatial structures which are at the limit of numerical resolution. Nevertheless, Fig. 1 shows clearly the high kurtosis levels near the wall, which is the object of this study.

B. Events determining the high kurtosis level

In order to explore the background of these high kurtosis levels, we first determine in our DNS database the values that contribute most to the kurtosis. It turns out that these are events, primarily associated with very large velocity fluctuations of say $|v'/v_{\mathrm{rms}}| > 10$. An example of such an event is given in Fig. 2. The events appear to be very rare, i.e. they cover only about 0.04 % of the horizontal plane. Further-

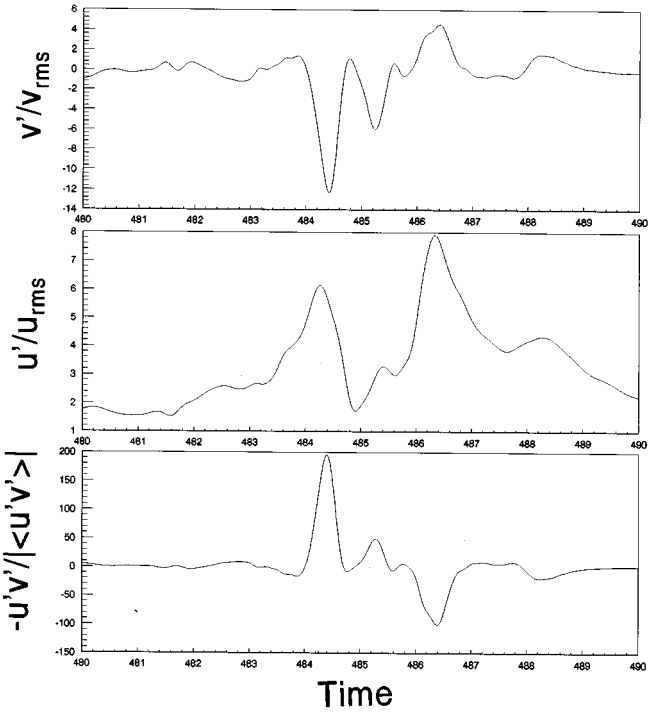

FIG. 2. Trace of a selected event at $y^+=2.54$ as function of time made dimensionless with U_m and H; given are (a) the v fluctuation non-dimensionalized with $v_{\rm rms}$, (b) the u fluctuation non-dimensionalized with $u_{\rm rms}$, and (c) the instantaneous Reynolds stress uv non-dimensionalized with the mean Reynolds stress at the same height.

more, they only occur in the vicinity of the wall and at higher levels, say for $y^+>\sim 10$, such large velocity excursions in terms of $|v'/v_{\rm rms}|$ are no longer found.

From 6 independent realizations of the flow field, we have selected 10 events based on the criterion that each event includes at least two points at $y^+=1.3$ for which the magnitude of $|v'/v_{\rm rms}|>10$. For the moment we shall indicate these events as velocity spikes. To study the flow field around such a velocity spike in more detail, we have considered a region with dimensions $\Delta x^+\approx 400$, $\Delta y^+\approx 173$, and $\Delta z^+\approx 200$ that is centered around the selected points where $|v'/v_{\rm rms}|>10$. The flow fields of all events were found to possess some common characteristic properties which we will illustrate here with help of a typical example.

In Fig. 3 we show the contour plots of $v'/v_{\rm rms}$ and

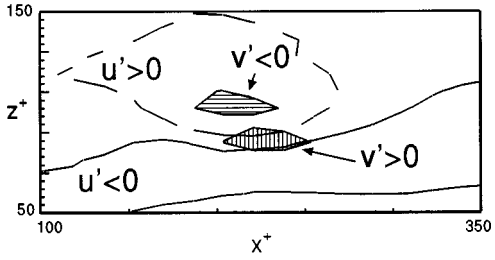

FIG. 3. Contour plot of $v'/v_{\rm rms}$ (horizontally hatched area: $v'/v_{\rm rms}<-5$ and vertically hatched area: $v'/v_{\rm rms}>5$) and of $u'/u_{\rm rms}$ (solid line: $u'/u_{\rm rms}<-1$ and dashed line: $u'/u_{\rm rms}>1$) for a typical high kurtosis event at $y^+=1.3$.

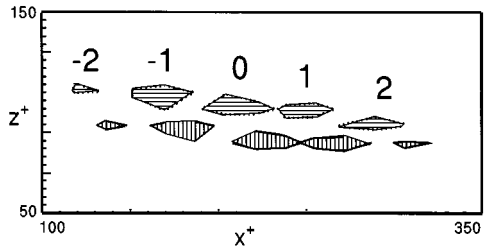

FIG. 4. The time evolution of velocity spikes indicated by contour plots of $v'/v_{\rm rms}$ (horizontally hatched pattern $v'/v_{\rm rms}<-6$ and vertically hatched pattern $v'/v_{\rm rms}>6$) at $y^+=1.3$, where the numbers indicate time sequence: the number 0 corresponds with the time instant of Fig. 3; the time separation between the numbered events is $0.4h/U_m$.

$u'/u_{\rm rms}$ of this typical event in the (x,z)-plane at $y^+=1.3$. The horizontally hatched area has $v'/v_{\rm rms}<-5$ (further referred to as a *negative velocity spike*) and the vertically hatched area is the area with $v'/v_{\rm rms}>5$ (further referred to as a *positive velocity spike*). In addition, we show in this figure a high-speed region with $u'/u_{\rm rms}>1$ (indicated by the dashed line) and a low-speed region with $u'/u_{\rm rms}<-1$ (indicated by the solid line).

Figure 3 illustrates the following general properties that we have found for a high kurtosis event. First, an event can be characterized by a positive and negative velocity spike which always appear in pairs. Second, the region covered by each spike measures about 50 wall units in the streamwise direction and 30 wall units in the transverse direction. Finally, the negative velocity spike is always located in a high-speed area which means that it can be characterized as a strong sweep, whereas the positive velocity spike is usually located in between a high- and low-speed region.

The time evolution of the velocity spikes is illustrated in Fig. 4 which shows contour plots of $v'/v_{\rm rms}$ in the (x,z)-plane at $y^+=1.3$. The numbers in the figure indicate time instants which have been taken at an interval of $0.4H/U_m$. The mean life-span of the spike-pair is thus found to be about $2H/U_m$.

We must realize that these velocity spikes appear only very close to the wall, i.e. in the viscous sublayer where one may expect that local dynamics is governed by the viscous time scale, ν/u_τ^2. This time scale in our case measures $\sim 0.1H/U_m$. We thus find that the spikes survive for about 20 viscous time scales and this means that their dynamics should be related to phenomena outside the viscous sublayer. This fact is corroborated by the propagation speed of the spikes which is $0.6-0.7U_m$ and which is much larger than the mean velocity at $y^+=1.3$ which is $0.08U_m$.

Having suggested that the spikes must be related to turbulence phenomena outside the viscous sublayer, we proceed to collect more evidence to support this result. To this end we show in Fig. 5 velocity vectors plotted on a transverse $(y-z)$ plane at $x^+=203$ that passes through the centre of the negative velocity spike indicated by the arrow. We notice two strong streamwise vortices located at position $y^+\simeq 32$, $z^+\simeq 46$ (indicated by the letter B) and at position $y^+\simeq 95$, $z^+\simeq 38$ (indicated by A). Another streamwise vortex close to

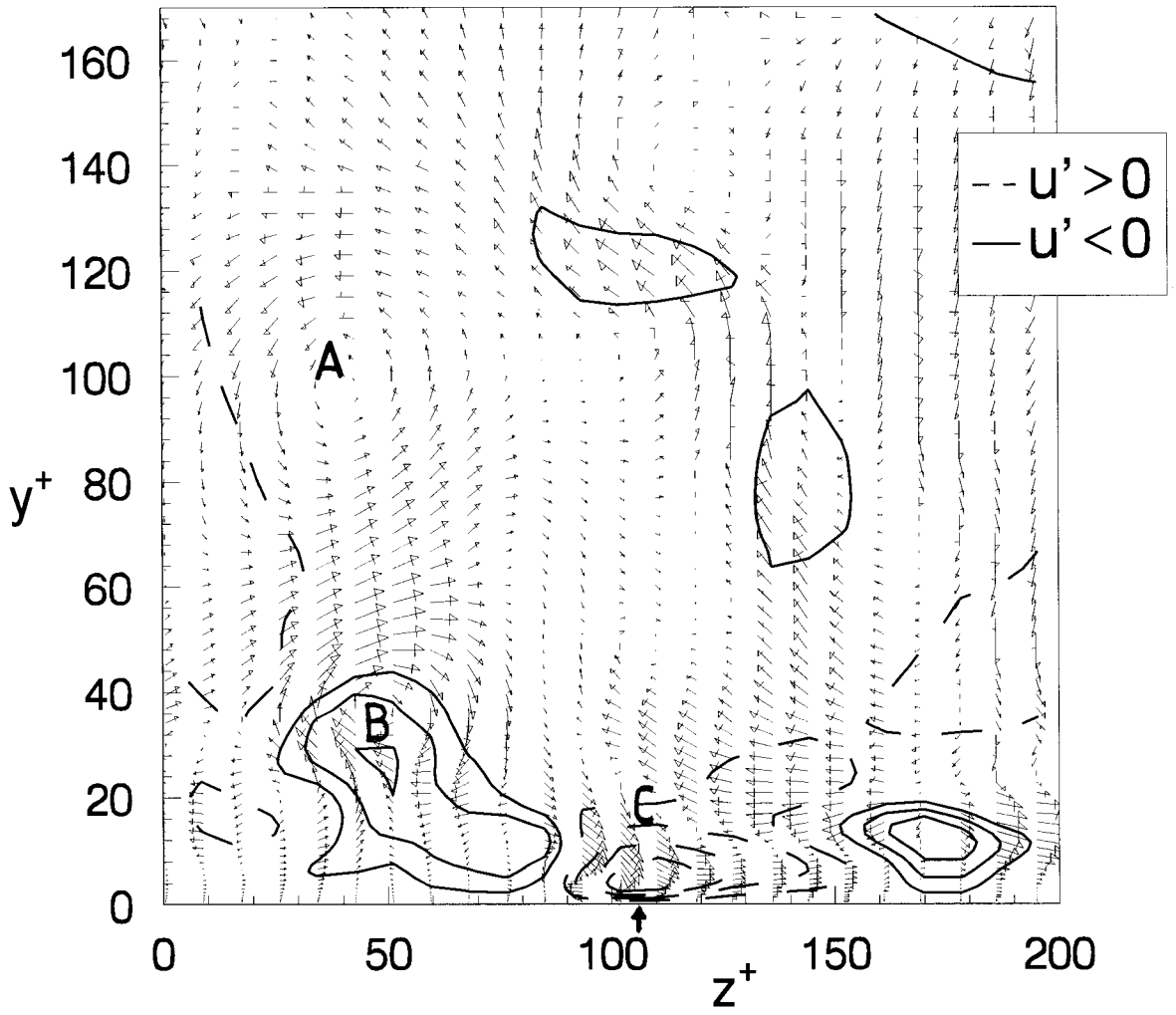

FIG. 5. Velocity vector plot on the $y-z$ plane at a $x^+=203$ which dissects the negative velocity spike, indicated by the arrow; the letters indicate streamwise vortices; the isolines illustrate contours in which either $u'>0$ (dashed lines) or $u'<0$ (solid lines).

the wall, indicated by the letter C, is found at the position $y^+\simeq 15$, $z^+\simeq 120$. Because of its closeness to the wall, the velocity between vortex C and the wall is strongly amplified due to the contribution of the mirror vortex. In addition the no-slip boundary condition at the wall leads to creation of vorticity of the opposite sign, which Brooke and Hanratty[11] call the vortex regeneration process. Aside, we may note that the vortex regeneration process is perhaps also responsible for the vortex C as a result of the interaction of vortex B with the wall. Fig. 5 shows that the vortex regeneration process involving vortex C results in a strong downwash velocity in the direction of the wall: our negative velocity spike.

According to Brooke and Hanratty the vortex regeneration process is also associated with high levels of the Reynolds stress. This agrees with our results. Figure 5 shows that areas with $u'>0$, indicated by the dashed lines, coincide with the strong negative v' and this clearly results in a strong contribution to the Reynolds stress.

The outcome of this discussion is that the large velocity spikes which are responsible for the high kurtosis of the normal velocity fluctuations, are found to be related to the vortex regeneration process described by Brooke and Hanratty.[11] In this process, the near-wall vortex C, which itself is possibly the result of interaction of vortex B with the wall, causes a strong downwash which impinges on the surface. The result is a strong negative velocity spike, which at the same time is related to a strong sweep motion. The height of vortex C has been estimated as $y^+\simeq 15$. The mean velocity at this height is $U/U_m\simeq 0.7$ and this agrees reasonably well with the propagation speed which we can estimate from Fig. 4. So the long lifetime of our spike event is most probably related to the persistence of vortex C in the flow region above the viscous sublayer and this explains why the dynamics of our spike event is not determined by the viscous time scale.

III. EXPERIMENT

A. Description

To verify the explanation for the high kurtosis events given in the previous section, we have carried out some experiments which were designed especially for observation of strong negative velocity spikes. The experiments were done in a pipe flow facility with a length 34 m and a diameter 40

TABLE I. Turbulence statistics of the measured time series of the axial velocity fluctuations, u', and the normal fluctuations v' in wall units, i.e. non-dimensionalized with u_τ and ν.

	$y^+=5$		$y^+=30$	
	u'	v'	u'	v'
Mean	6.0	0.026	14.1	0.06
rms	2.1	0.23	2.4	0.8
Skewness	0.53	−0.2	−0.38	−0.2
Kurtosis	2.9	6.8	2.8	4.1
$\overline{u'v'}$	0.13		0.78	

mm. The fluid used is water. The measurements were performed with 2-D LDV system manufactured by Dantec. A special measuring section was used to avoid refraction through curved pipe walls of the laser beams, which distorts the position of the LDV measuring volume. It consists of a rectangular box filled with water in which the pipe wall has been replaced by a thin foil. The foil has almost the same refraction index as water. This measuring box makes it possible to obtain reliable velocity measurements at a distance of 0.2 mm from the wall which in our case amounts to 3.1 plus units. For more details on the experimental setup and the measuring procedure we refer to den Toonder.[12]

Measurements were made of the axial (x) and the normal (y) velocity components at the Reynolds number $\mathrm{Re}=U_m D/\nu=10018$ (U_m being the bulk mean velocity in the pipe and D the diameter) or $\mathrm{Re}_\tau=u_\tau D/\nu=624$. It was not possible to carry out reliable experiments at the low Reynolds number for which the direct simulations were performed. However, we do not consider this to be a problem because as we will see below, the best we can hope for is only a qualitative comparison between experimental and numerical simulation data. Therefore, experimental data taken at a small but not necessarily equal Reynolds number seem to be sufficient.

We consider the measurement data taken at two positions, namely at the non-dimensional distances $y^+=5$ and 30 from the pipe wall. At each of these measurement positions, time series of instantaneous velocity observations were taken. At $y^+=5$, 221270 samples were gathered in 284 s and at $y^+=30$, 165456 samples in 75 s. The macroscopic time scale of the turbulence is estimated to be $D/U_m=0.16$ s. Hence the measurement at $y^+=5$ consisted of 1775 time scales, while the measurement at $y^+=30$ lasted 470 time scales.

B. Results

In Table I we show some statistics of the observed time series. It must be noted that the accuracy with which these quantities could be computed is not very large, because of the short duration of the measurements. Using the estimate given in Lumley and Panofsky[13] the statistical error amounts to 0.9 % for the mean velocity in the $y^+=5$ measurement, while for the position $y^+=30$ this error is 1.7 %. The errors made in the higher-order statistics will be much larger and we will return to this below.

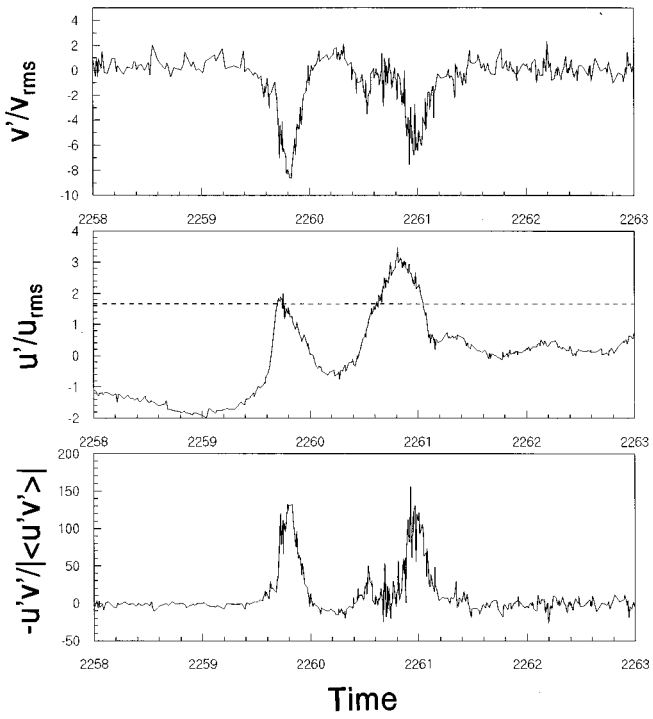

FIG. 6. A negative velocity spike as function of non-dimensional time, measured with LDV in a turbulent pipe flow, at $y^+=5$; time evolution of normal velocity (upper figure); streamwise velocity (middle figure); Reynolds stress (lower figure). The dashed line corresponds to $0.6U_m$.

The data series were examined for events with the same signature as the high kurtosis event of the DNS database that we have discussed in Section II. So we look for peaks or spikes in the measured velocity signal. As a criterion for such spikes we specify that at least two samples have a magnitude larger than 8 times the rms value of the total series (note that in Section II we took $|v'/v_{\mathrm{rms}}|>10$ but this was at $y^+=1.3$). At this stage, a peak can in principle be either positive (i.e., larger than the mean) or negative (i.e., smaller than the mean).

With the above criterion two velocity spikes were found for the time series at $y^+=5$, both negative. One of these is depicted in Fig. 6 (upper figure) where the normal velocity component is shown as function of time, non-dimensionalized with U_m and $D/2$. In Fig. 6 we find a less strong negative velocity spike that immediately follows the large one but according to our criterion this smaller peak is not selected as an event. The width of the velocity spike, defined as the width at the point where the value of the signals equals 5 times the rms, equals 14 ms. In Section II we found that the length of a spike region with $|v'|>5v_{\mathrm{rms}}$ is about 50 wall units long and that the spikes propagate at a speed of about $0.65U_m$. This leads to a passing time of such a structure past a fixed point of $77\nu/(u_\tau U_m)$. For our pipe flow, this value corresponds to a passing time of 20 ms and this agrees reasonably well with our measured value. Furthermore, Fig. 6 (middle figure) shows the axial fluctuating velocity with a positive peak that almost exactly coincides with the negative normal velocity spike and which thus re-

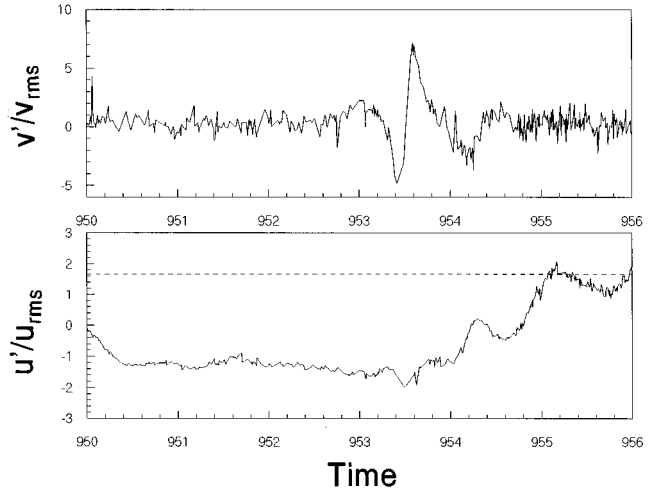

FIG. 7. A positive spike as measured with LDV in a turbulent pipe flow at $y^+=5$; time evolution of normal velocity (upper figure); streamwise velocity (lower figure). The dashed line corresponds to $0.6U_m$.

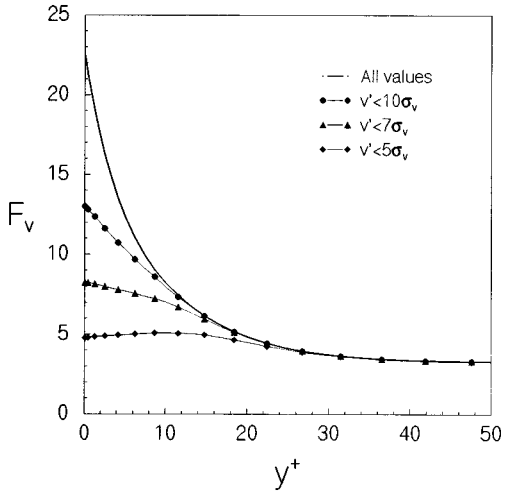

FIG. 8. DNS results for the near-wall kurtosis of the normal velocity fluctuations where the velocity fluctuations above a certain value (in terms of the local rms value) have been omitted.

sults in a very large instantaneous Reynolds stress shown in the lower figure of Fig. 6.

Our experimental results seem therefore to be consistent with the picture given in section II. To limit ourselves to the main points, we have found that the existence of very strong negative velocity spikes is confirmed and it is clear that the value of the kurtosis will be strongly increased by such events. Furthermore, the velocity spikes are transported with a high speed relative to the local axial velocity (the dashed line in the middle figure of Fig. 6, e.g., indicates the value of $0.6U_m$). Finally, the velocity spikes are accompanied by a large instantaneous Reynolds stress. More or less the same results were found for the second spike in our time series, which we therefore will not show here.

As mentioned above, no positive velocity spikes were detected. The largest positive peak in the normal velocity is depicted in Fig. 7 (upper figure). The corresponding axial fluctuating velocity is shown in Fig. 7 (lower figure), and shows no correlation with the normal velocity peak. Hence, there is no contribution to the turbulent shear stress as we have found in the case for the negative spikes. These results largely agree with the DNS data. In other words, the velocity spikes that contribute to the high kurtosis levels are connected to strong sweeps.

There were no spikes found in the axial velocity signal. The value of this signal relative to its mean value did not even exceed five times the rms value and this seems consistent with the moderate values of the kurtosis, which is for the axial component close to the Gaussian value of 3.

The time series for $y^+=30$ showed no spikes at all, neither positive nor negative. All peaks in this series, relative to the mean value, stay below 6 times the rms value.

As a conclusion we may state that our experiment has confirmed that the high kurtosis events in the normal velocity fluctuations, found in the DNS database of section II, can be connected to strong sweeps. These sweep events are found only quite close to the wall and they are possibly related to the vortex regeneration process described by Brooke and Hanratty.[11] The appearance of the spikes is rare, i.e. in our data series they occur only ~ 0.01 % of the time. Furthermore, in our one-point measurements their duration is short due to a high transport velocity (which does not exclude the possibility that the spikes themselves have a long lifetime as we found in the DNS results). Finally, the contribution of such a negative velocity spike to the Reynolds stress seems to be very large.

One may wonder why previous experiments have failed to observe these velocity spikes. To explain this fact, we first note that these previous experiments were in general not designed to observe such spikes. A reliable observation of spikes requires a good time resolution and also a large measuring range. To begin with the time resolution, in our case we have collected data near the wall at a rate of approximately 1 kHz, whereas in other experiments the data rate is usually much smaller, e.g. Durst *et al.*[9] mention a value of 100 Hz for their measurements near the wall. Even with a small data rate one would still measure occasionally the large velocities due to the spikes but given the small time period in which the spike is advected past the instrument, an event would result only in a very small number of such observations. Such a small number of very large values may be easily interpreted as a measuring error. For instance, Durst *et al.*[9] interpret all observations beyond 7 rms as error and these values are consequently removed from the observations. However, such a removal of high values will influence the kurtosis strongly. This is illustrated in Fig. 8, where we show the DNS data for the kurtosis after removal of velocity fluctuations which exceed a certain threshold in terms of the rms value.

However, even in the case when we would not remove any values from the observed data, it would still be very difficult to obtain a reliable observation for the kurtosis due to the statistical error in the observations. To show this we estimate the measuring error Δ_4 for the fourth central moment $\overline{x^4}$ which is given by

$$\Delta_4^2 = \frac{\overline{x^8} - \overline{x^4}^2}{N},$$

where N is the number of independent observations. Let us assume for the probability density of the stochastic variable x the following expression:

$$p(x) = \frac{p_0}{\sqrt{2\pi}} e^{-x^2/2} + p_1[\delta(x-x_1) + \delta(x+x_1)],$$

where the δ-functions indicate peaks superposed on a Gaussian distribution with unit variance. We take for the values of these peak $x_1 = 10$. Furthermore, we take for the frequency of occurrence of the peaks $p_1 = 0.00025$. For convenience we have taken the peaks to be symmetric with respect to $x = 0$ so that all odd central moments are zero. It not difficult to compute the even central moments with as a result $\overline{x^2} = 1.05$, $\overline{x^4} = 8.00$, and $\overline{x^8} = 50105$. The relative error in the fourth moment $(\Delta_4/\overline{x^4})$ is then given by $28/\sqrt{N}$. Even for a rather modest error, say 10%, the number of independent measuring samples required becomes very large and this results in impractically or sometimes even impossibly long measuring times. We should mention here that the kurtosis values given in Table I were obtained with a rather short measuring period and consequently have a large statistical error. For that reason these values have not been not entered in, e.g., Fig. 1.

One may perhaps wonder why the DNS data are able to produce the high kurtosis levels. The most probable reason in our opinion is that the turbulence statistics computed from the DNS data are based on surface averages which have in general a better statistical accuracy than line averages.

Based on the results presented in this paper, we feel confident that the high kurtosis values for the normal velocity fluctuations, previously found only in DNS results, occur indeed in real turbulent flows and moreover, they seem to be connected with the existence of coherent structures, viz. strong sweeps, near the wall.

IV. CONCLUSIONS

Analyzing a DNS data base for channel flow and an experimental data base obtained in a turbulent pipe flow, we have found that high values of the kurtosis of the normal velocity fluctuations near the wall are caused by events that are very rare in space and time. These events are characterized by spikes in the time series with a large negative values. They have a large propagation speed relative to the local mean velocity. It seems that a spike event with a negative normal velocity appears together with a weaker spike which has a positive normal velocity component and which propagates at the same speed. These spikes appear only close to the wall, i.e. $y^+ < 15$ and they seem to survive for more than 20 viscous time scales.

The negative spikes appear to have a large contribution to the Reynolds stress so that they can be characterized as strong sweeps. The positive spike has no significant contribution to the Reynolds stress. The negative spike structure can be associated with a strong downwash towards the wall due to a streamwise vortex in the buffer layer in a process known as vortex regeneration.

The large normal velocities in these spikes which can exceed $|v'/v_{\mathrm{rms}}| = 10$, make their experimental observation difficult and this explains why experiments up to now have never measured high values of the kurtosis near the wall. The fact that the high kurtosis levels are found in DNS data, is probably connected to the fact that statistics in DNS are based on surface averages. Nevertheless, it is clear that the spikes contribute significantly to the higher-order moments of the normal velocity fluctuations and therefore it is important that they are included in any computation or observation of these statistics.

ACKNOWLEDGMENTS

This work was partly carried out while the first author was a visitor at the laboratory of Aero and Hydrodynamics and partly while the third author was a visitor at the Department of Engineering Mechanics. Both authors wish to acknowledge the financial support made available by the two universities involved within the context of a Chinese/Dutch academic collaboration programme. We also acknowledge the support of NWO-NCF in providing computer time on the Cray-YMP. Finally we would like to mention the financial support for the second author by NWO-FOM and for the first and fourth author by NNSFC in the context of the project on turbulence research.

[1] J. W. Brooke and T. J. Hanratty, ''Origin of turbulence-producing eddies in a channel flow,'' Phys. Fluids A **5**, 1011 (1993).
[2] J. Kim, P. Moin, and R. Moser, ''Turbulence statistics in a fully developed channel flow at low Reynolds number,'' J. Fluid Mech. **177**, 133 (1987).
[3] P. R. Spalart, ''Direct simulation of a turbulent boundary layer up to $R_\theta = 1410$,'' J. Fluid Mech. **187**, 61 (1988).
[4] S. L. Lyons and T. J. Hanratty, ''Large-scale computer simulation of fully developed turbulent channel flow with heat transfer,'' Int. J. Num. Methods Fluids **12**, 999 (1991).
[5] R. Kristoffersen and H. I. Andersson, ''Direct simulations of low Reynolds number turbulent flow in a rotating channel,'' J. Fluid Mech. **256**, 163 (1993).
[6] S. Gavrilakis, ''Numerical simulation of low-Reynolds-number turbulent flow through a straight square duct,'' J. Fluid Mech. **244**, 101 (1992).
[7] J. G. M. Eggels, F. Unger, M. H. Weiss, J. Westerweel, R. J. Adrian, R. Friedrich, and F. T. M. Nieuwstadt, ''Fully developed turbulent pipe flow: A comparison between direct numerical simulation and experiment,'' J. Fluid Mech. **268**, 175 (1994).
[8] R. I. Karlsson and T. G. Johansson, ''LDV measurements of higher-order moments of velocity fluctuations in a boundary layer,'' in *Laser Anemometry in Fluid Mechanics III*, edited by R. J. Adrian, T. Asanuma, D. F. G. Durao, F. Durst, and J. H. Whitelaw, Lisbon, Portugal, pp. 273–289, 1988.
[9] M. A. Niederschulte, R. J. Adrian, and T. J. Hanratty, ''Measurements of turbulent flow in a channel at low Reynolds numbers,'' Exp. Fluids **9**, 222 (1990).
[10] F. Durst, J. Jovanovic, and J. Sender, ''LDA measurements in the near-wall region of a turbulent pipe flow,'' J. Fluid Mech. **295**, 305 (1995).
[11] H. P. Kreplin and H. Eckelmann, ''Behaviour of the three fluctuating velocity components in the wall region of a turbulent channel flow,'' Phys. Fluids **22**, 1233 (1979).
[12] J. M. J. den Toonder, ''Drag reduction by polymer additives in a turbulent pipe flow: laboratory and numerical experiments,'' Ph.D. thesis, Delft University of Technology, 1996.
[13] J. Lumley and H. A. Panofsky, *The Structure of Atmospheric Turbulence* (Wiley–Interscience, New York, 1964).